

Fig. 5.25: Daily variation of discharge from the Podroteja spring.

The estimated mean altitudes of the catchment areas of the given springs are in agreement with the altitudes calculated by the $\delta^{18}\text{O}$ -values of the yearly variation (see chapter 5.1.4).

5.2. DISSOLVED INORGANIC CARBON ISOTOPE COMPOSITION OF WATERS

(J. URBANC, B. TRČEK, J. PEZDIČ, S. LOJEN)

The objective of this research is to determine whether the isotope composition of TDIC in water and the chemical composition of water in the outflow from a karst aquifer can be used to interpret the carbon isotope composition and partial pressure of soil CO_2 in the aquifer's recharge area. Further, an attempt was made to establish which model of carbonate rock dissolution in water can be applied to interpret initial conditions and define the degree of accuracy with which the initial conditions can be described if the only data available are those of the isotopic and chemical composition of water in the outflow from a carbonate aquifer. Thus, in our research, the carbon isotope composition and partial pressure of soil CO_2 measured in the recharge area of a karst aquifer were compared to the values, calculated from the isotopic and chemical composition of water in the outflow from aquifer.

Previous observations have shown that the formation of soil CO_2 is to the greatest extent conditioned by soil temperature (BILLES et al. 1971; DORR & MUNNICH 1980; KIEFER & BROOK 1986; WOOD et al. 1993), by the

quantity of organic matter in the soil (WOOD et al. 1993) and by soil moisture (KIEFER & BROOK 1986). Most of soil CO₂ passes into the atmosphere, only a minor part of the total CO₂ is washed into the ground by precipitation (WOOD & PETRAITIS 1984; QUADE et al. 1989; HENDRY et al. 1993). Soil CO₂ can originate from the decomposition of organic matter or root respiration (WOOD & PETRAITIS 1984; HENDRY et al. 1993; DUDZIAK 1994).

Some investigations indicate that during carbonate dissolution in soil, the solution equilibrates with soil CO₂. Thus this is an open system of carbonate dissolution (REARDON et al. 1979; QUADE et al. 1989), while indications for the closed system of carbonate dissolution in the soil were also present (DEINES et al. 1974).

5.2.1. Carbon Isotope Composition In Individual Parts Of The Researched System

The carbon isotope composition of water in the outflow from aquifer can be influenced by the carbon isotope compositions of soil CO₂, carbon isotope composition of the carbonate rock, and by potential changes of carbon isotope composition of water resulting from isotope exchange between the carbon from atmospheric CO₂ and the carbon degassing from water CO₂.

5.2.1.1. Characteristics of carbon isotope composition of soil CO₂

Several sampling points underlying different vegetation covers and at different altitudes were chosen for the measurement of isotope composition and partial pressure of soil CO₂. Three probes for the sampling of soil CO₂ were placed in a forest with prevailing beeches: in the Belca valley (sampling point with the lowest altitude), near Podkraj, and data obtained at Obli Vrh at an altitude of about 1000 m were also included in the investigation. The probes at Col and Grgar were located in soil underlying grass. The probe for the sampling of soil CO₂ in a spruce forest was located near Podkraj.

Samples of soil CO₂ were taken using metal capillaries with an inside diameter of 1 mm, which were dug about 50 cm deep into the ground. Samples of soil atmosphere were transferred into preevacuated 0.7 l glass ampoules. In the laboratory, atmospheric CO₂ was isolated according to the usual procedure (CRAIG 1953) and its isotope composition was measured on the Varian Mat 250 mass spectrometer. From the quantity of isolated CO₂ and the volume of the ampoule the concentration of CO₂ in the gas sampled was calculated.

Dissolved inorganic carbon from water was extracted by adding concentrated H₃PO₄ acid to the water in vacuum (MOOK 1970).

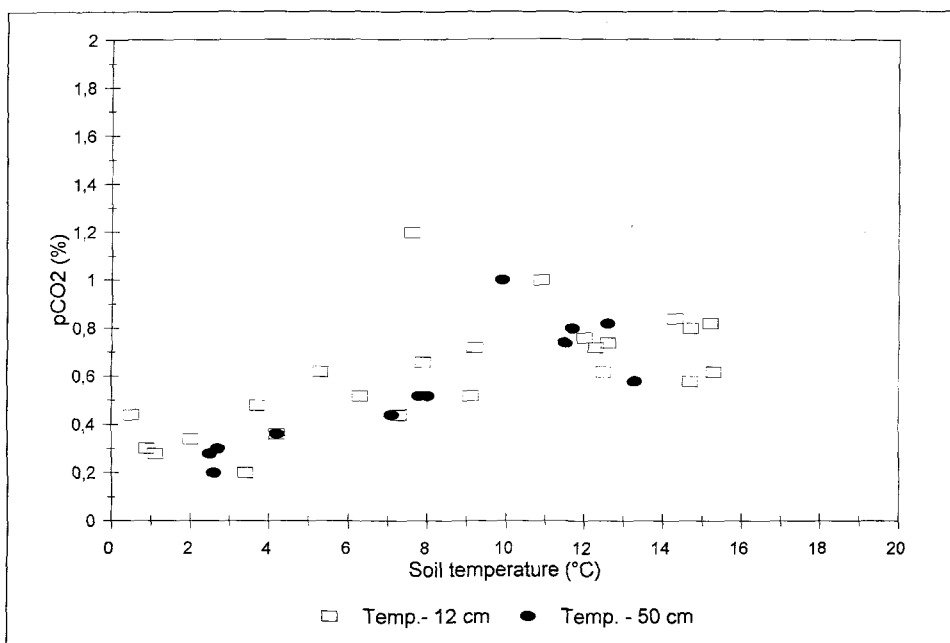


Fig. 5.26: Relation between soil temperature and partial pressure of soil CO₂ in beech forest.

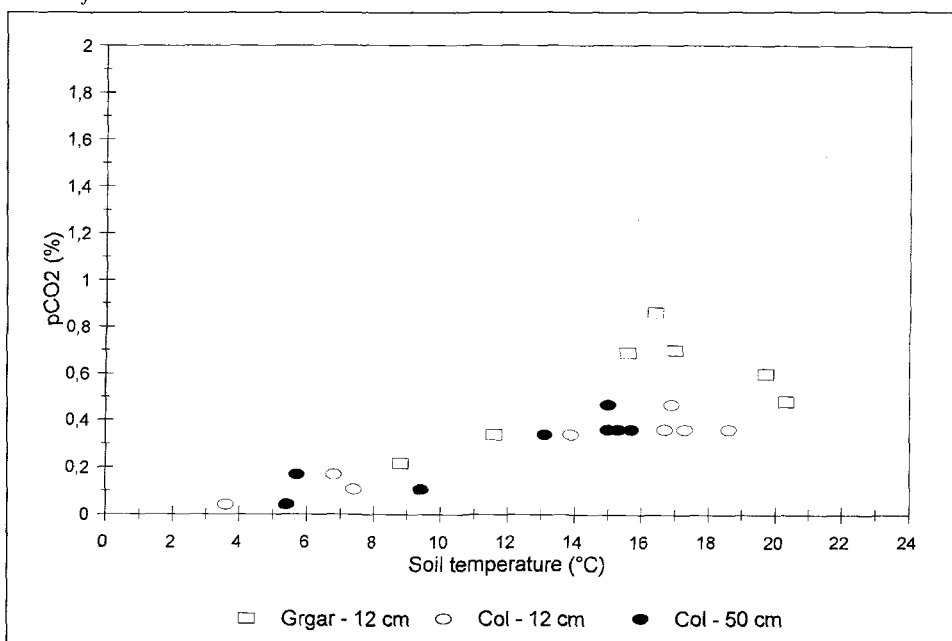


Fig. 5.27: Relation between soil temperature and partial pressure of soil CO₂ in soil under grass.

A linear correspondence between temperature and partial pressure of soil CO₂ can be clearly observed (Fig. 5.26, 5.27). Compared to the soil underlying beech forest, the soil overlaid with grass has lower partial pressures of soil CO₂. The smaller generation of CO₂ is of course conditioned by a smaller transition of organic matter into the soil overlain with grass.

Fig. 5.28 shows average partial pressures measured at individual locations, compared to the average soil temperature. Values measured at sampling points located under the same type of vegetation lie along the same line, and the inclination of P_{CO₂}-T correlation lines for beech and grass is also similar.

Beech forest is the prevailing vegetation in the research area, therefore the majority of carbon isotope composition values and partial pressures of CO₂ were measured in soil underlying beech forest. Monthly measurements of soil CO₂ carbon isotope composition showed that most of the δ¹³C values lie between -17 and -23 ‰ (Fig. 5.29), while partial pressures of CO₂ range between 0.07 to 1.2 % of the total atmospheric pressure.

A certain interdependence between the carbon isotope composition and partial pressure of soil CO₂ is evident from Fig. 5.28. Such correlation could result from the mixing of biogenic carbon, originating from the decomposition of organic matter in the soil, with the carbon from atmospheric CO₂. In this case, the ratio between biogenic carbon and atmospheric carbon can be expressed by the mixing equation:

$$\delta^{13}C_t = \frac{\delta^{13}C_b \cdot P_b + \delta^{13}C_a \cdot P_a}{P_t} \quad (11)$$

P ... partial pressure
a ... atmospheric
b ... biogenic
t ... total

In the mixing model, the following δ¹³C concentrations were adopted: -23 ‰ for organic carbon, -8 ‰ for atmospheric carbon (KEELING et al. 1979), and 0.03 ‰ for the partial pressure of atmospheric CO₂. The curve of the mixing model is given in Fig. 5.29, indicating that modelled results are in good correlation with the values measured. Equation 11 was statistically proved, the test statistic F = 3.7+10⁻⁹ (TRČEK 1996). Thus it can be concluded that fluctuations in carbon isotope composition of soil CO₂ can be to a great extent attributed to the mixing of biogenic and atmospheric carbon.

In the above case, sampling points were located under the same type of plant, namely under beech. A different carbon isotope composition of biogenic carbon is to be expected in soil zones underlying other types of vegetation. Figure 5.30 shows the relation between the carbon isotope composition and

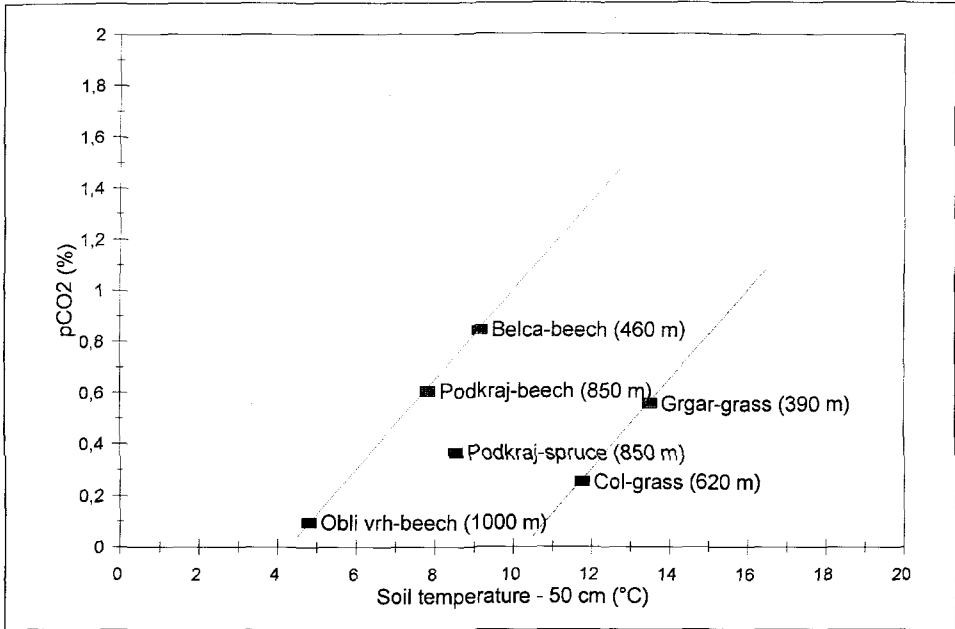


Fig. 5.28: Mean soil temperatures of different locations related to the mean partial pressure of CO_2 .

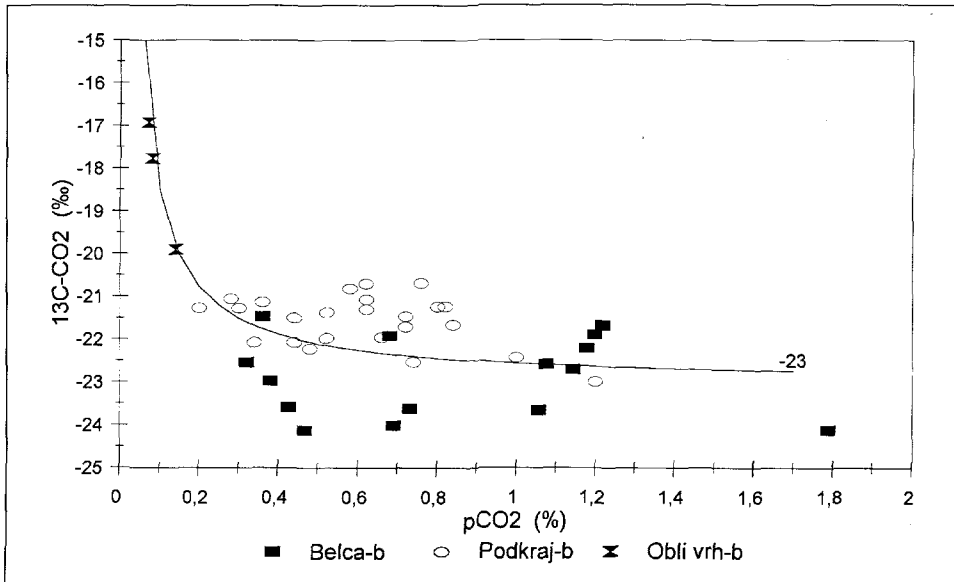


Fig. 5.29: Relation between partial pressure of soil CO_2 and its carbon isotope composition for soil in beech forest.

partial pressure of soil CO₂ for all types of vegetation covers sampled. It can be seen that samples from spruce forest show no significant deviation from the properties of CO₂ in beech forest, while more considerable differences are observed in soils under grass covers. The samples taken from soil underlying grass near Col have a more negative isotope composition of biogene soil CO₂ of about -24 ‰, while the samples from Grgar show a distinctly more positive isotope composition of the biogene component, about -21.5 ‰. This difference in the carbon isotope composition of soil CO₂ under the same type of vegetation is attributed to the different altitude and the different mean soil temperatures. The sampling point near Grgar is situated at an altitude of 390 m in rather Mediterranean climatic conditions, and that near Col is at 620 m above the sea level, where climatic conditions are much harsher. The prevailing types of grass in warmer areas are those with the Hatch-Slack (C4) cycle which generates more positive δ¹³C values in plant tissues. On the other hand, the Calvin cycle (C3) prevails in grass from colder areas, giving more negative δ¹³C values of plant tissues (CERLING 1984).

Thus it can be concluded that in the area of the Trnovsko-Banjška Planota, CO₂ with varying isotopic properties enters the ground: the most negative values of biogenic carbon isotope composition are to be expected in CO₂ from soil underlying grass and from higher-lying and colder areas (about -24 ‰), soils underlying beech or spruce forests tend to have somewhat more enriched δ¹³C values of biogenic carbon (about -23 ‰), and grass from warmer and lower areas give the most positive initial isotopic signal (about -21.5 ‰).

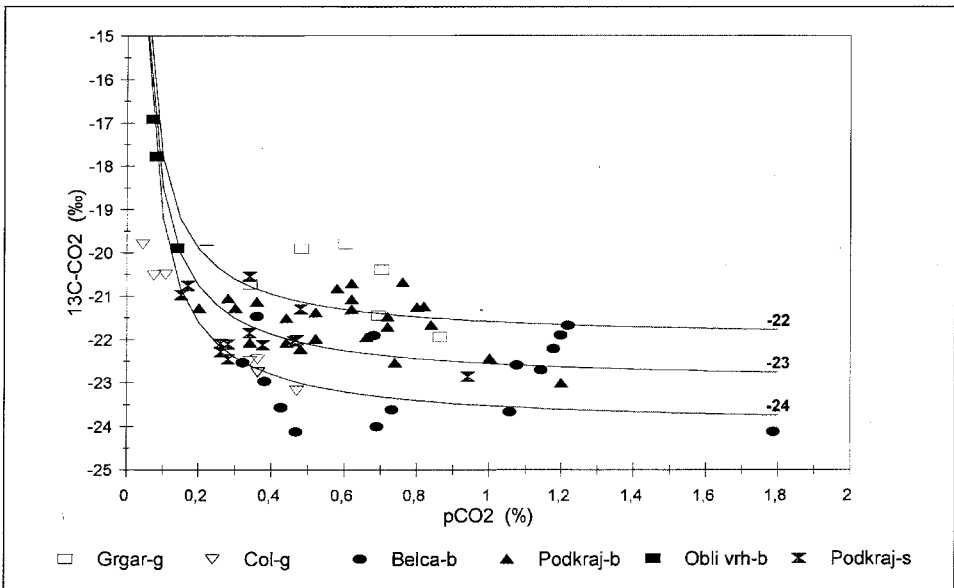
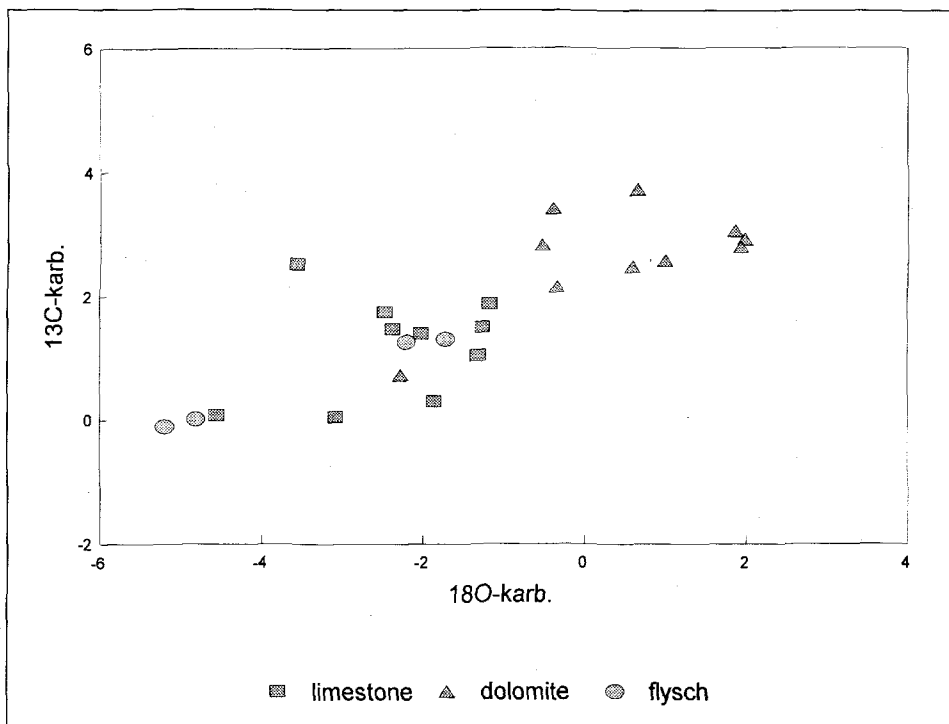


Fig. 5.30: Relation for all investigated soil types.

5.2.1.2 Carbon isotope composition of carbonate rocks

The research area is for the most part composed of Mesozoic limestones and dolomites and flysch rocks. In all, 24 rock samples were taken for isotopic analyses. Measurements of carbon isotope composition of observed samples showed a range in $\delta^{13}\text{C}$ values between 0 and +4 ‰ (Fig. 5.31). It can be observed on the graph that dolomites have mostly more enriched $\delta^{13}\text{C}$ and $\delta^{18}\text{O}$ values compared to limestones or flysch.



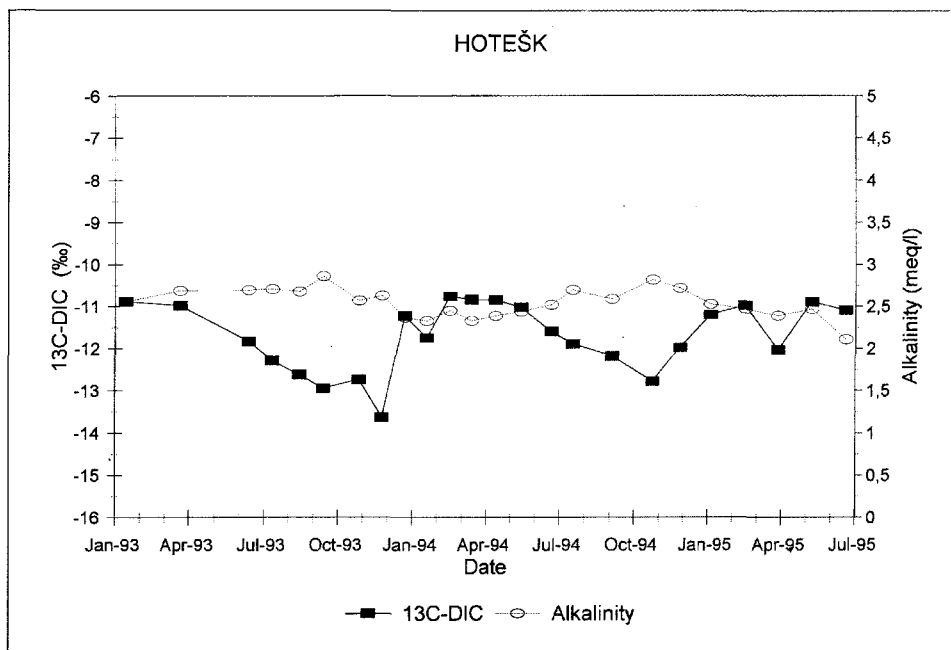


Fig. 5.32: Carbon isotope composition and alkalinity of Hotešk spring.

place until spring, and a gradual depletion in $\delta^{13}\text{C}$ values follows over the entire year to the late fall minimum.

Such seasonal isotopic variability can be explained in the following way: Due to the correlation between pedotemperature and partial pressure of soil CO_2 , the gradual increase of soil temperature over the year results in an increased production of soil CO_2 . In the fall, soil temperatures are the highest, organic matter enters the ground due to lost leaves, which results in a maximum in soil CO_2 partial pressure. A higher content of the biogenic component in soil CO_2 is reflected also in the carbon isotope composition, which reaches its most depleted $\delta^{13}\text{C}$ values, and in the DIC isotope composition in the outflow, where the most depleted $\delta^{13}\text{C}$ values were also detected.

Lower soil temperatures in winter considerably hinder the processes of soil CO_2 generation, consequently the soil atmosphere contains a higher percentage of atmospheric CO_2 with more positive $\delta^{13}\text{C}$ values. When the water from melted snow penetrates the soil in spring recharge area, a larger quantity of atmospheric carbon enters the system, resulting in enriched $\delta^{13}\text{C}$ values in the outflow.

A similar pattern of seasonal fluctuations can be perceived also in the other springs, except in the Hubelj, which shows a distinctly different $\delta^{13}\text{C}$ isotopic curve (Fig. 5.33).

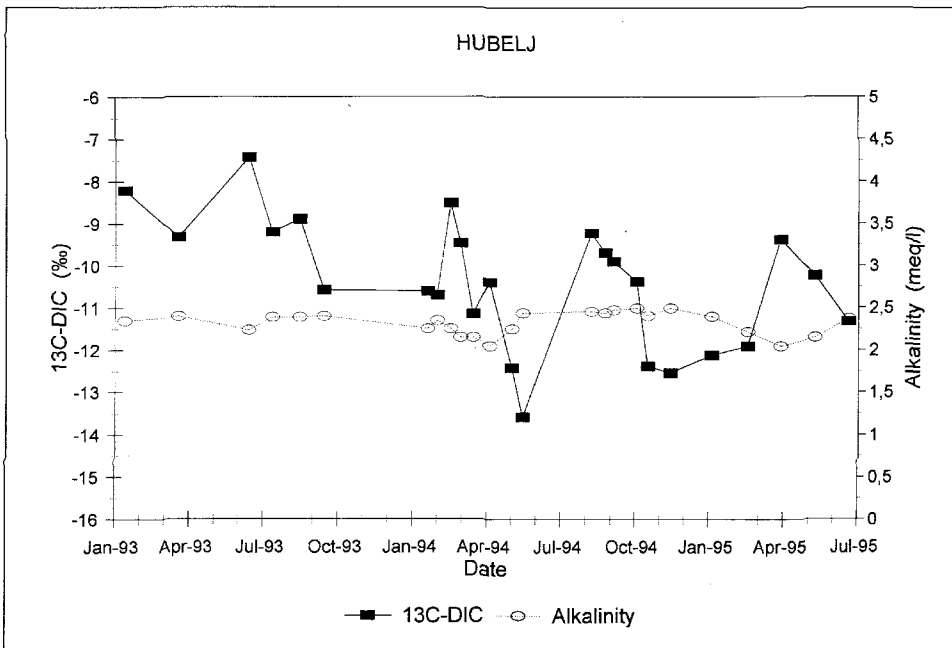


Fig. 5.33: Carbon isotope composition and alkalinity of Hubelj spring.

A comparison of carbon isotope composition variation amplitudes in the outflow is also very interesting. The springs Vipava (Fig. 5.34), Podroteja (Fig. 5.35), Hotešk (Fig. 5.32) and Prelesje (Fig. 5.38) show a fairly similar range of yearly $\delta^{13}\text{C}$ values at about 2.5 ‰. Yearly fluctuations of the carbon isotope signal are much larger in the Hubelj, where the amplitude of $\delta^{13}\text{C}$ values from spring 1993 to spring 1994 was over 6 ‰ (Fig. 5.33). This indicates that Hubelj has a higher aquifer water exchange rate, resulting in a less pronounced dampening of the isotope signal. A fairly large range in the isotope signal was measured also in samples from Mrzlek spring, however, the large variability can in this case be attributed to a stronger influence of the Soča river and the fact that Soča river water is more enriched in the heavier carbon isotope (Fig. 5.36).

During surface flow, isotope exchange between the DIC and atmospheric carbon takes place. Because atmospheric carbon is enriched in the heavier carbon isotope, a change towards the more positive $\delta^{13}\text{C}$ values can be expected.

Most of the samples for the 7th SWT project were taken from springs, yet some of them were also taken from lower course of surface flow, e.g. from streams on flysch rocks and from river Soča. In order to evaluate the scope of isotope exchange, sampling was carried out along the Bela stream above

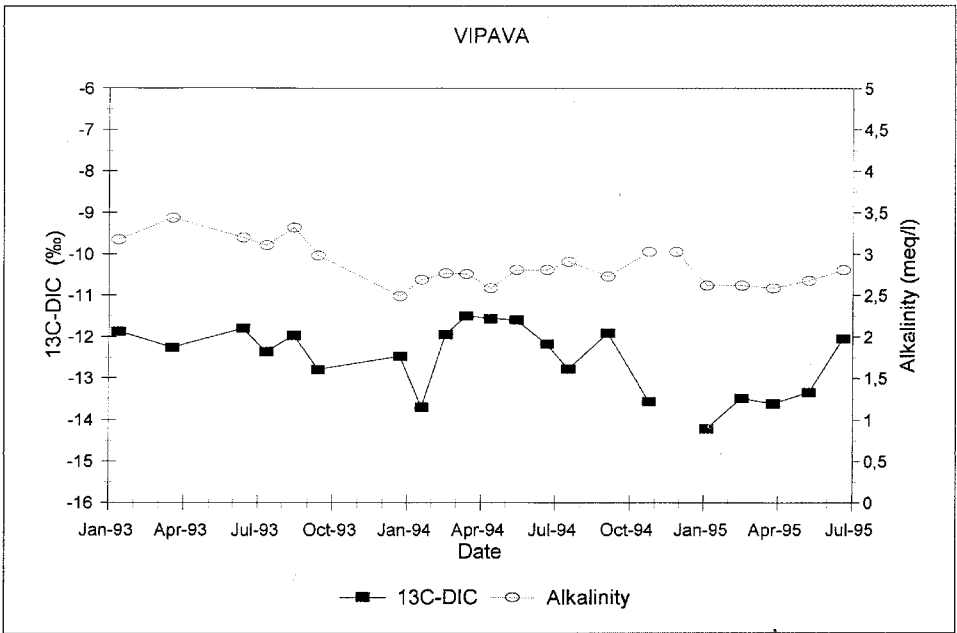


Fig. 5.34: Carbon isotope composition and alkalinity of Vipava spring.

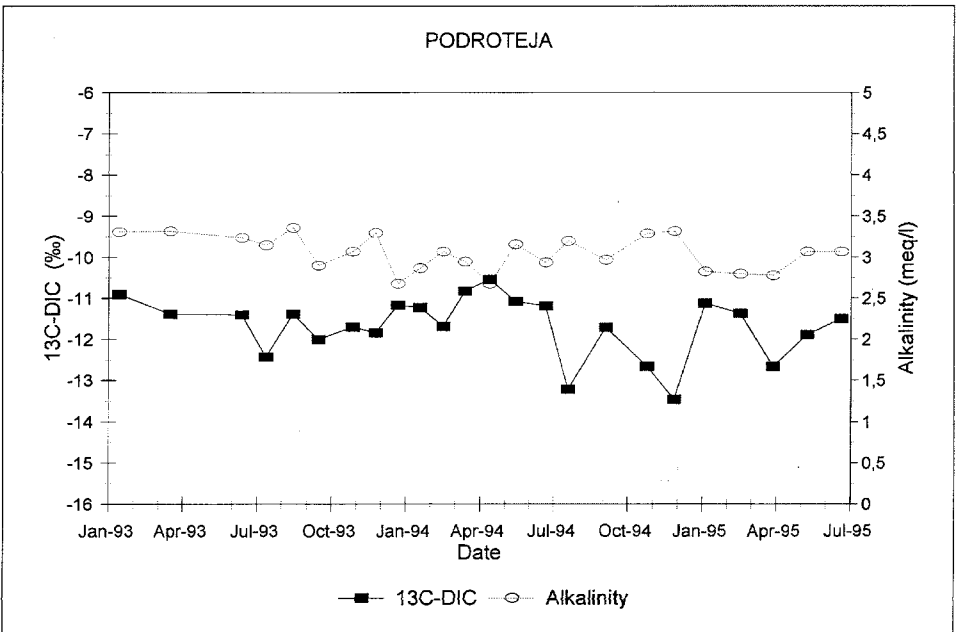


Fig. 5.35: Carbon isotope composition and alkalinity of Podroteja spring.

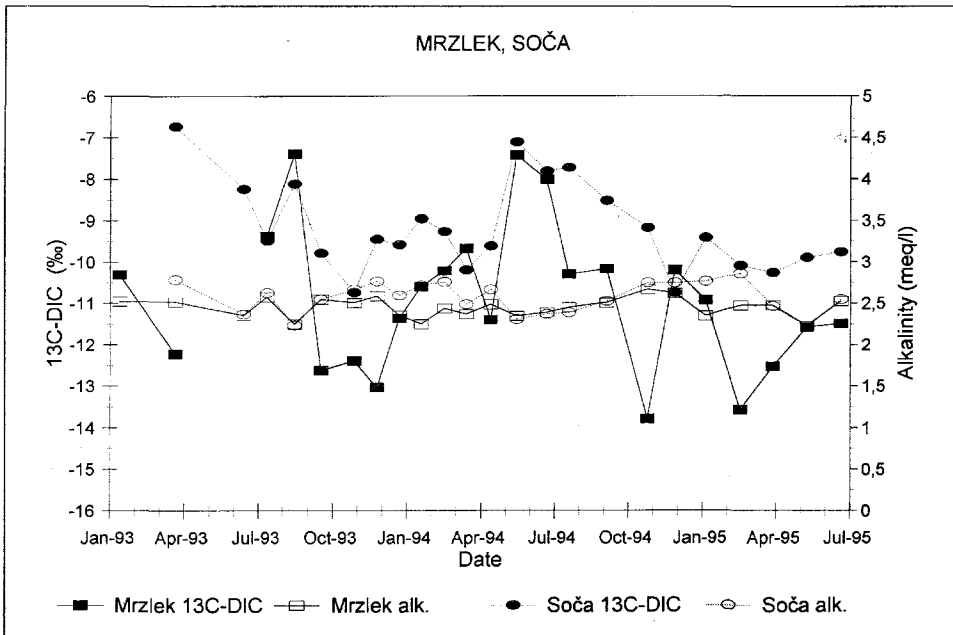


Fig. 5.36: Carbon isotope composition and alkalinity of Mrzlek and Soča springs.

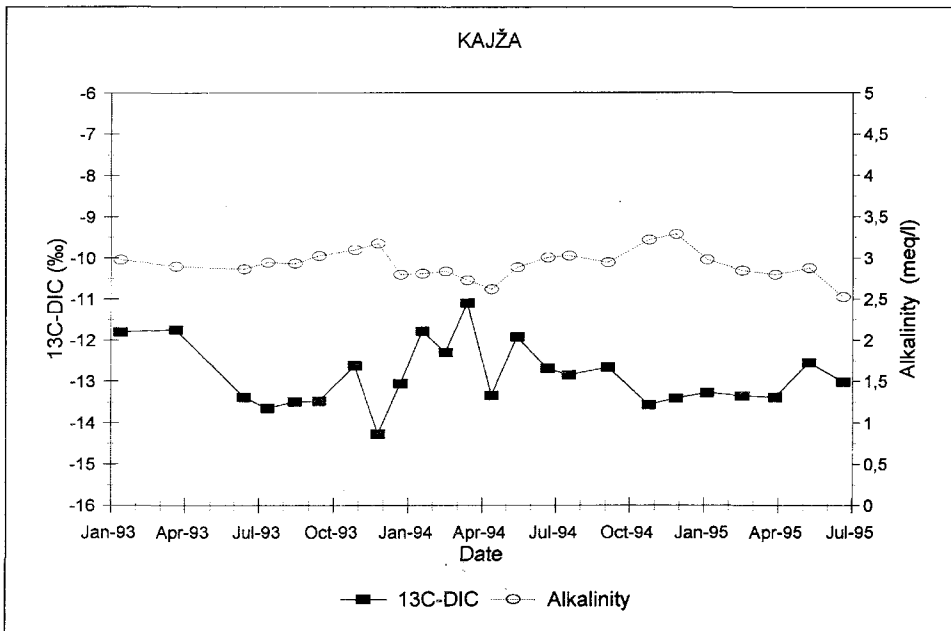


Fig. 5.37: Carbon isotope composition and alkalinity of Kajža spring.

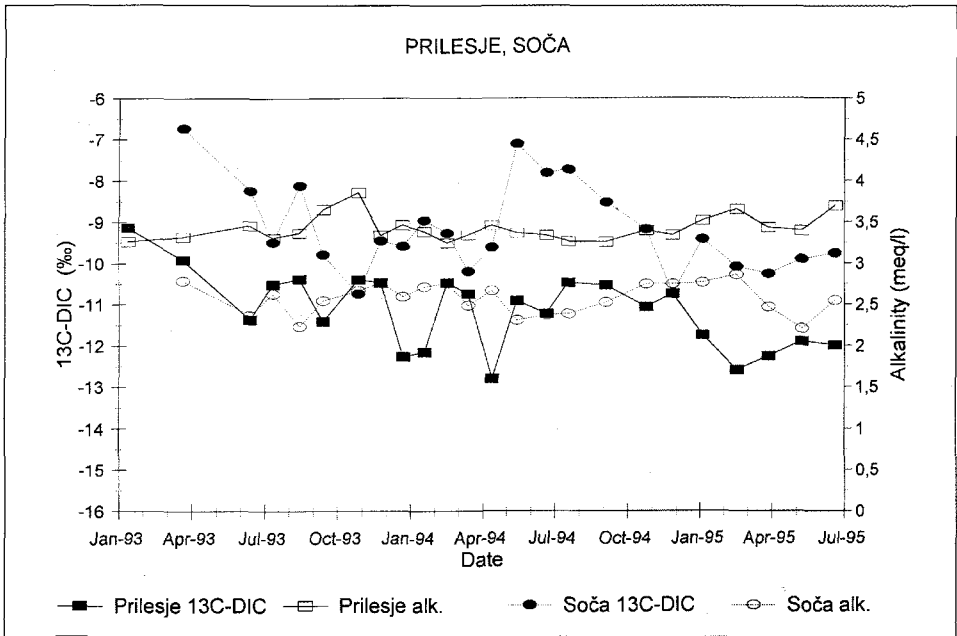


Fig. 5.38: Carbon isotope composition and alkalinity of Prelesje and Soča springs.

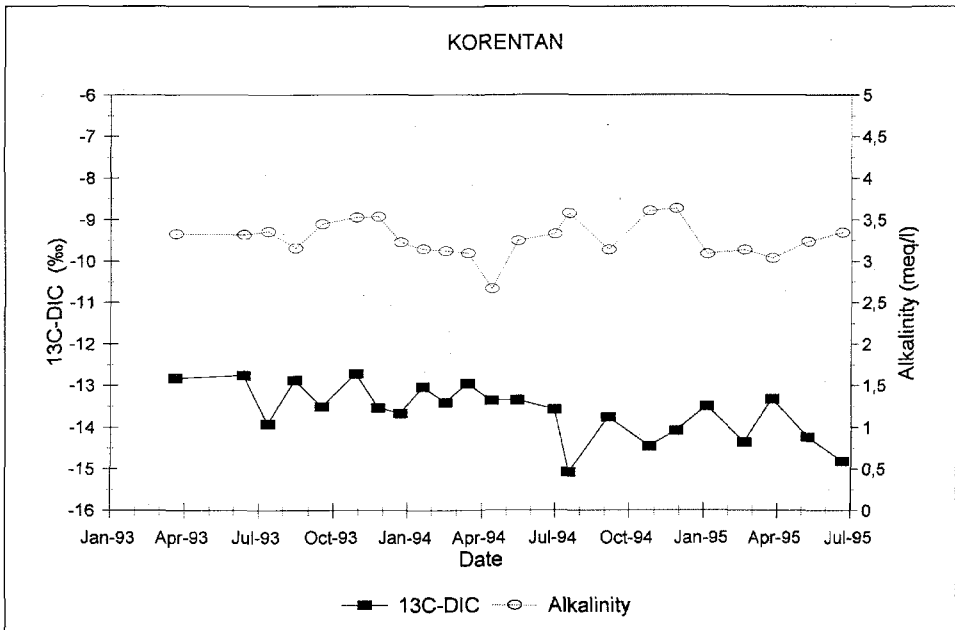


Fig. 5.39: Carbon isotope composition and alkalinity of Korentan spring.

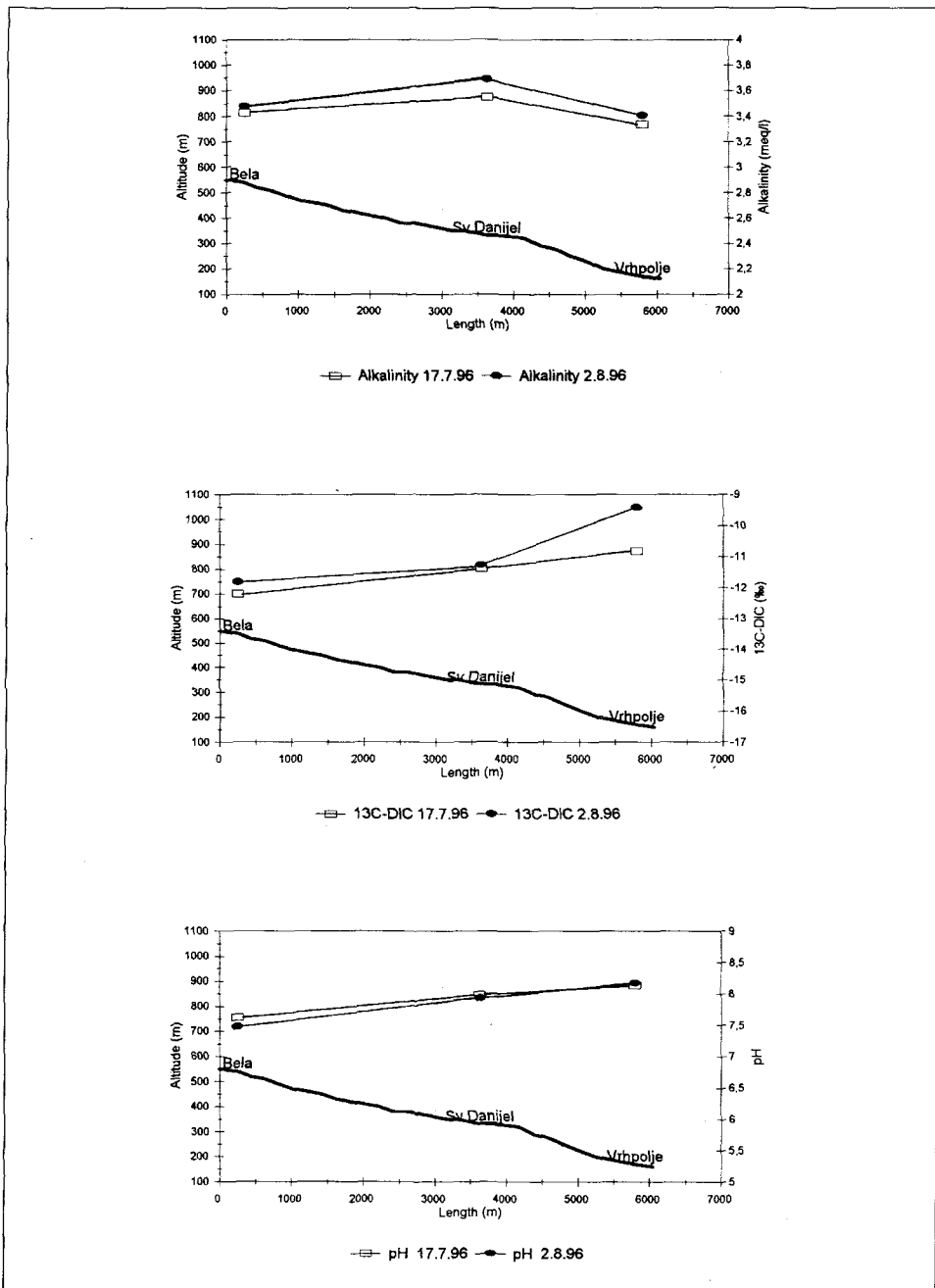


Fig. 5.40: Changes of alkalinity, $\delta^{13}\text{C}$ DIC and pH along the surface flow course of the Bela.

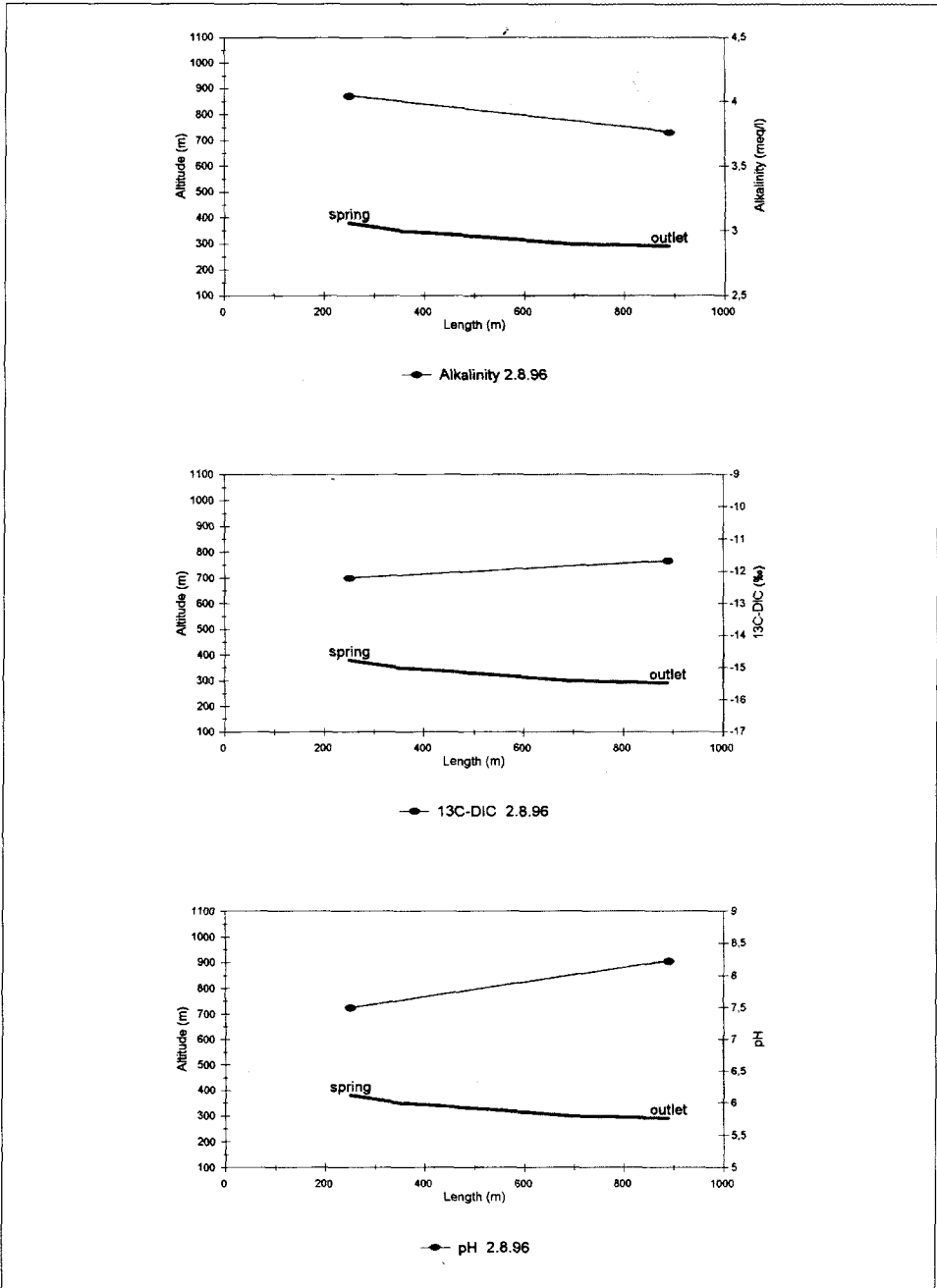


Fig. 5.41: Changes of alkalinity, $\delta^{13}\text{C}$ DIC and pH along small stream near Sveti Danijel.

Vipava. Three sampling points were selected: at the village Bela, at Sv. Daniel and at the village Vrhpolje. Fig. 5.40 illustrates the changes in the carbon isotope composition, pH and alkalinity of water along its surface flow course. Indeed, an increase in $\delta^{13}\text{C}$ values was observed along the course of the surface flow, which indicates isotope exchange between the carbon from atmospheric CO_2 and the carbon from DIC. A more distinct influence of isotope exchange was measured at low water level on 2.8.1996, when the isotope composition of water between the villages Bela and Vrhpolje changed by as much as 2.4 ‰. The same isotope effect was measured also in the stream flowing into the Bela above Sv. Daniel, which was monitored along its entire course (Fig. 5.41). Thus it can be concluded that significant increases in $\delta^{13}\text{C}$ values can take place in surface streams, due to the isotope exchange between atmospheric carbon and the carbon from hydrocarbonate. This is a fact to be taken into account in the interpretation of isotope measurements.

The relationship between alkalinity and the isotopic content of the DIC is very interesting (Fig. 5.42). The majority of results are distributed in the form of a long cloud; higher alkalinity corresponds to DIC depleted in ^{13}C . Such distribution of results can be explained by the fact that higher alkalinity of water requires higher initial partial pressures of soil CO_2 , and the concentration of $\delta^{13}\text{C}$ depleted carbon in the soil air is increased at higher partial pressures of soil CO_2 .

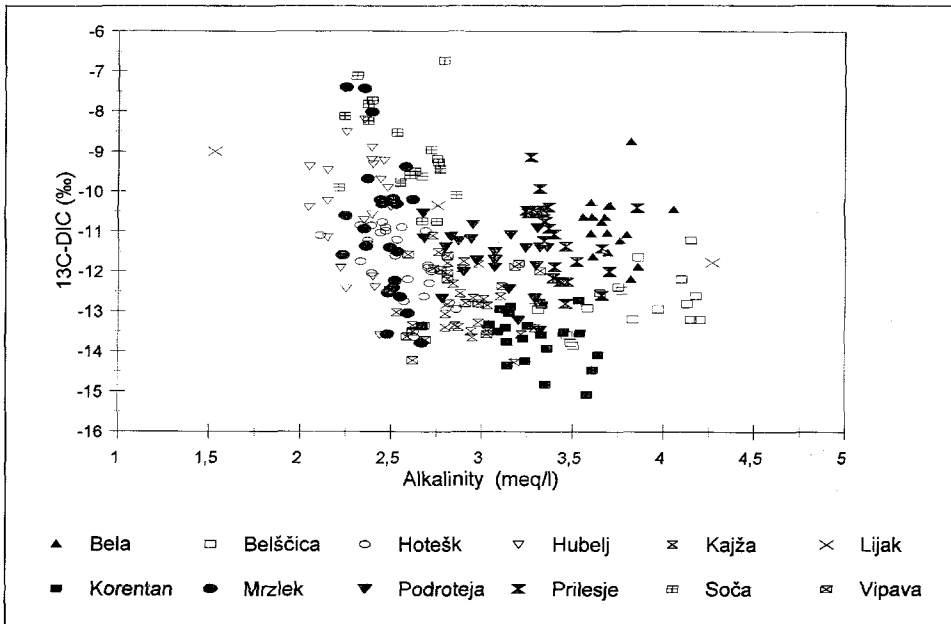


Fig. 5.42: Relationship between alkalinity and $\delta^{13}\text{C}$ DIC of the waters from investigation area.

It is also evident from Figure 5.42 that the Bela and the Prelesje distinctly deviate from the basic principle. Bela stream is recharged in flysch rocks, thus this deviation of the $\delta^{13}\text{C}$ values towards more positive values can be explained by the effect of isotope exchange between the DIC and atmospheric carbon during surface flow. We assume that water with partially changed $\delta^{13}\text{C}$ values due to surface flow enters also into the Prelesje water supply well.

5.2.2. Reconstruction of Initial CO_2 Isotope Composition

The carbon isotope composition of DIC reflects isotopic processes during the dissolution of atmospheric and soil CO_2 in water and in the neutralisation of aggressive water with the carbonate rock. These processes are described with the open and closed system models.

a) The Open System Model

According to the open system model, the carbon isotope composition of an equilibrated solution can be described with the equation (HENDY 1971):

$$\delta^{13}\text{C}_t \cdot [\text{DIC}] = \delta^{13}\text{C}_{\text{H}_2\text{CO}_3} \cdot [\text{H}_2\text{CO}_3^*] + \delta^{13}\text{C}_{\text{HCO}_3} \cdot [\text{HCO}_3^-] + \delta^{13}\text{C}_{\text{CO}_3} \cdot [\text{CO}_3^{2-}] \quad (12)$$

The carbon isotope composition of individual ion species can be expressed also:

$$\delta^{13}\text{C}_{\text{HCO}_3} = \delta^{13}\text{C}_{\text{CO}_2} + \epsilon_{\text{HCO}_3} \quad (13)$$

ϵ ... isotope enrichment of a species with regard to CO_2 .

From equations 12 and 13 the isotope composition of initial soil CO_2 can be derived:

$$\delta^{13}\text{C}_{\text{CO}_2} = \frac{\delta^{13}\text{C}_t \cdot [\text{DIC}] - \epsilon_{\text{H}_2\text{CO}_3} \cdot [\text{H}_2\text{CO}_3^*] - \epsilon_{\text{HCO}_3} \cdot [\text{HCO}_3^-] - \epsilon_{\text{CO}_3} \cdot [\text{CO}_3^{2-}]}{[\text{H}_2\text{CO}_3^*] + [\text{HCO}_3^-] + [\text{CO}_3^{2-}]} \quad (14)$$

b) The Closed System Model

According to the closed system model, the carbon isotope composition of a solution can be expressed by the closed system mass balance equation (DEINES et al. 1974):

$$\delta^{13}\text{C}_t \cdot [\text{DIC}] = \delta^{13}\text{C}_{\text{CO}_2} \cdot [\text{CO}_2 \text{ o}] + \delta^{13}\text{C}_c \cdot [\text{C}_c] \quad (15)$$

$\text{CO}_2\text{ o}$... the concentration of CO_2 in water before reaction with the carbonate rock

c ... carbon from the carbonate rock

$$\delta^{13}\text{C}_{\text{CO}_2\text{ o}} = \frac{\delta^{13}\text{C}_t \cdot [\text{DIC}] + \delta^{13}\text{C}_c \cdot [\text{C}_c]}{[\text{CO}_2\text{ o}]} \quad (16)$$

$$\delta^{13}\text{C}_{\text{CO}_2} = \delta^{13}\text{C}_{\text{CO}_2\text{ o}} - \epsilon_{\text{CO}_2(\text{g}) - \text{CO}_2(\text{aq})} \quad (17)$$

The concentrations of carbon ion species in a carbonate solution were calculated using the geochemical program PHREEQE (PARKHURST et al. 1985).

Figure 5.43 gives a comparison of $\delta^{13}\text{C}$ values with partial pressures of input CO_2 ; values obtained from field measurements were compared with values calculated by means of the open and closed system models from data on the chemical and isotopic composition of water in the outflow from a karst aquifer. The $\delta^{13}\text{C}$ values calculated according to the open system model

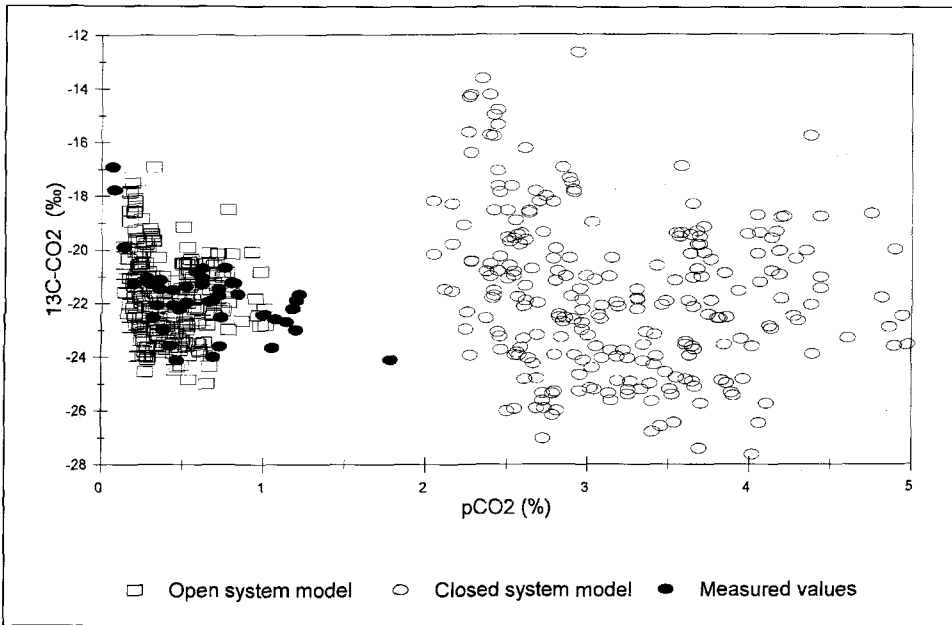


Fig. 5.43: Comparison of calculated and measured values of $\delta^{13}\text{C CO}_2$ and partial pressure of soil CO_2 in the recharge area of observed karst springs.

correspond relatively well to the $\delta^{13}\text{C}$ values and partial pressures of soil CO_2 obtained in measurements in karst aquifer recharge areas. We can see, that modelled results are fairly well comparable to the results obtained from measurements, making an interpretation of initial data on the basis of the chemical and isotope composition of water in the outflow generally possible. The dissolution of carbonates in the cases studied proceeds by open-system processes, where the solution during the neutralisation with the carbonate rock remains in contact with the soil CO_2 . In this process, the carbon isotope composition of soil CO_2 is equilibrated with that of the solution.

Fig. 5.44 gives a more detailed interpretation of the carbon isotope composition and the partial pressures of soil CO_2 , calculated according to the open system model from the DIC isotope composition and the water alkalinity of individual springs. The interpreted $\delta^{13}\text{C}$ values of soil CO_2 in the recharge areas mostly range between -17 and -25 ‰, and the interpreted partial pressures of initial CO_2 lie between 0.1 and 1% of the total atmospheric pressure. It has to be taken into account in the interpretation of results that water in the outflow is mostly highly homogenised, which can result in a considerably larger fluctuation of initial isotope compositions and partial pressures of soil CO_2 .

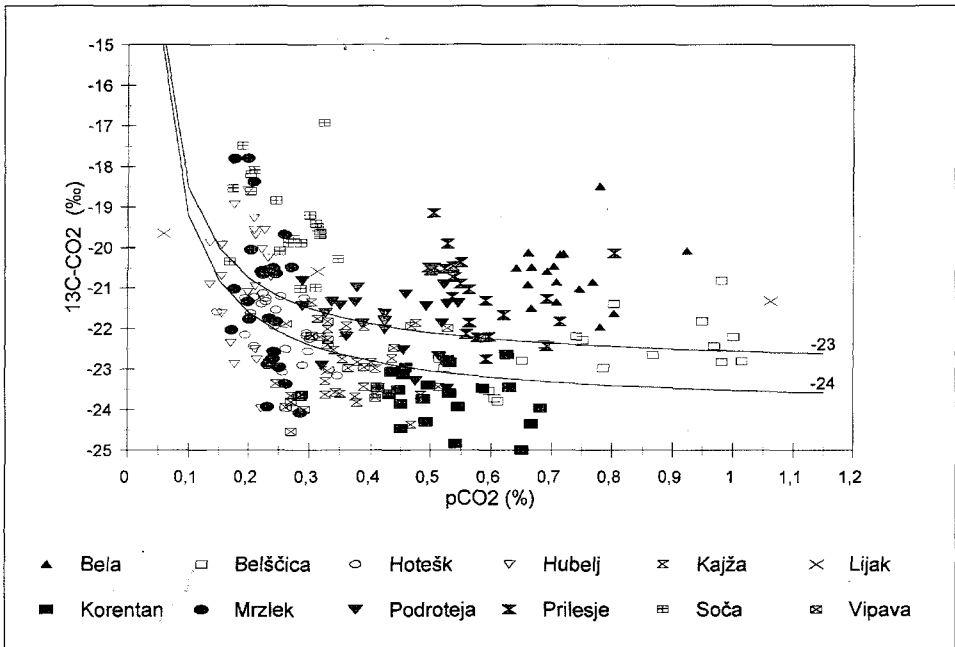


Fig. 5.44: Interpretation of $\delta^{13}\text{C}$ CO_2 and partial pressure of soil CO_2 on the basis of water $\delta^{13}\text{C}$ DIC and alkalinity.

Fig. 5.44 illustrates also considerable differences among individual springs as regards their carbon isotope compositions and initial CO₂ partial pressures. Similarly as in the δ¹³C DIC-alkalinity graph (Fig. 5.42), most of the data are distributed in the form of a cloud. This distribution can be relatively well explained by the mixing equation between the biogenic and atmospheric carbon in soil atmosphere (equation 11), where the adopted isotope composition of biogenic component of soil CO₂ is -24 ‰. In the majority of the results, the biogenic component isotope composition is in good accordance with the measurement results of soil CO₂ isotope composition, where the isotope composition of soil CO₂ biogenic component was estimated at about -23 ‰, using the mixing model.

The general trend in Fig. 5.44 is again not followed by the Bela and the Prelesje. This can be attributed to the effect of isotope exchange between the DIC and the carbon from atmospheric CO₂. Slight deviations from modelled values towards more positive values are present also in samples from the Belščica, Soča and Mrzlek. Due to the surface flow of the Soča and the Belščica, this deviation can be explained in the same way as in the Bela and the Prelesje. Deviations in the samples from the Mrzlek are caused by the presence of the Soča water in the Mrzlek samples at times of low water level.

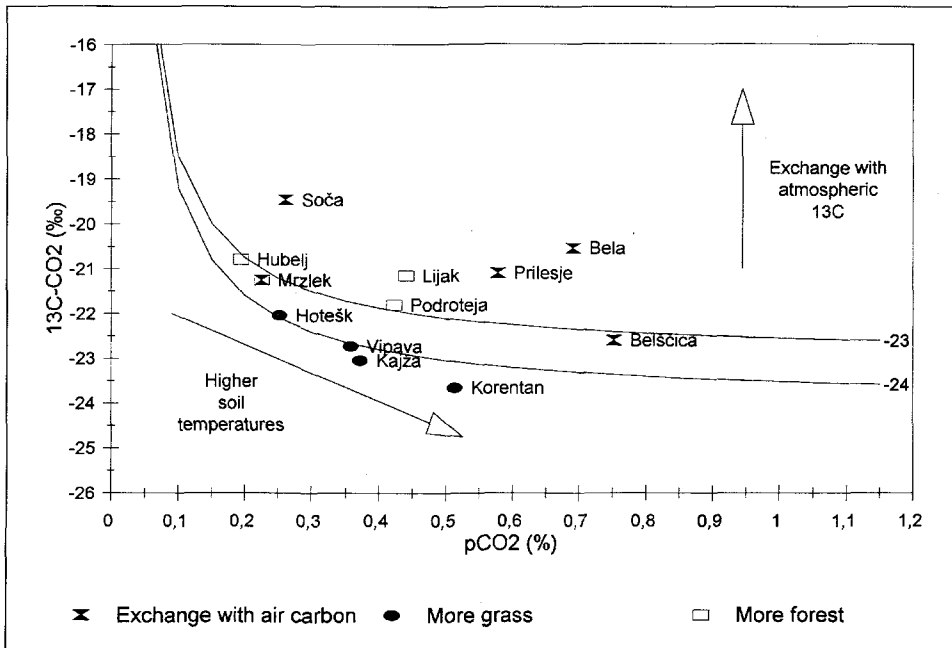


Fig. 5.45: Average values of δ¹³C CO₂ and partial pressure of soil CO₂ on the basis of water δ¹³C DIC and alkalinity.

Isotopic properties of individual springs are even more clearly evident from the graph of interpreted mean $\delta^{13}\text{C}$ values of soil CO_2 and its partial pressure (Fig. 5.45). The greater part of average values lie along theoretical curves of biogenic carbon -23 and -24 ‰. It is remarkable that springs with mainly forested recharge areas have average $\delta^{13}\text{C}$ values closer to the -23 ‰ curve, while the springs which recharge in areas underlying mainly grass, lie closer to -24 ‰. According to the data obtained from the regional forest management unit, grass areas amount to about 35 % at Banjščice, 25 % in the Nanos area, while they are negligible in the areas of Trnovski Gozd and Hrušica. The differences in the isotope composition of biogenic carbon therefore present a possibility of drawing conclusions about the vegetation properties of recharge areas. Adequate confirmation of these indications would of course require additional investigations.

On the basis of correlation between measured soil CO_2 partial pressure and soil temperature, and between the measured carbon isotope composition of soil CO_2 and soil temperature, and also on the basis of the influence of various types of vegetation on the measured carbon isotope composition and partial pressures of soil CO_2 , an attempt was made to approximately estimate mean values of soil temperature in recharge areas of individual springs (TRČEK 1997).

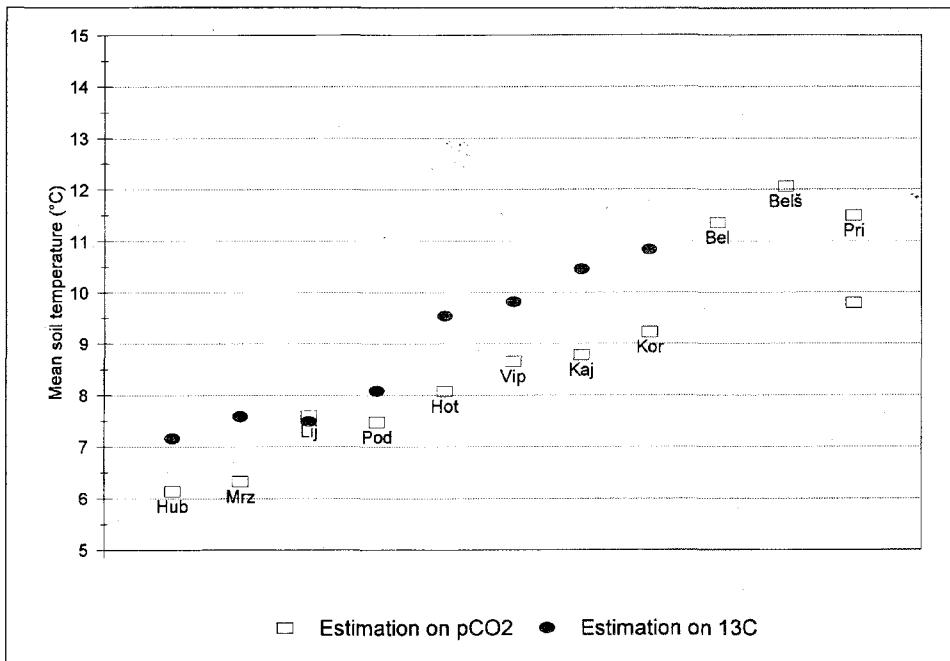


Fig. 5.46: Estimated mean soil temperatures of recharge areas on the basis of $\delta^{13}\text{C}$ CO_2 and partial pressure of soil CO_2 .

Calculations were made by two methods:

1. Average pedotemperatures were calculated on the basis of CO₂ partial pressure, obtained from the alkalinity of individual springs and taking into account the correlation between the measured partial pressure of soil CO₂ and soil temperature for approximate vegetation structure of the recharge areas.
2. Average temperatures were calculated from the DIC isotope composition, where the correlation between the measured carbon isotope composition of soil CO₂ and soil temperature for approximate vegetation structure of the recharge areas.

The estimated pedotemperatures are shown on Fig. 5.46. The effect of isotope exchange with atmospheric CO₂ was observed in the springs: Bela, Belščica and Prelesje, therefore their mean soil temperatures could only be estimated on a basis of CO₂ partial pressures.

5.3. SHORT-TERM INVESTIGATIONS DURING A HEAVY SNOWMELT EVENT (V. ARMBRUSTER, C. LEIBUNDGUT)

5.3.1. Introduction

A hydrograph separation of Hubelj and Vipava springs into event and pre-event water was done with the stable isotope ¹⁸O for a heavy snowmelt event in April 1996. The lighter meltwater made a hydrograph separation possible.

5.3.2. Methods

A two component mixing model was used for the hydrograph separation. In order to determine a representative isotope content of the snowmelt event water, a network of 10 snow lysimeters was put up in the catchment areas of Hubelj and Vipava springs in different altitudes. On the basis of the dependence of snowmelt water heights and isotope contents on altitude a weighting calculation was done and representative isotope contents for the two catchments were obtained.

5.3.3. Results and Interpretation

The field observation period lasted from March the 27th until April the 12th 1996. At the beginning of the period the karst plateaux were partly snow-covered. During a heavy precipitation event on April the 1st and 2nd (Fig. 5.47